Kinetics and Intermediates in the Autoxidation of Synthetic, Non-Porphyrin Iron(II) Dioxygen Carriers

Alexandra Sauer-Masarwa,[†] Norman Herron,[‡] Carol M. Fendrick,[‡] and Daryle H. Busch*[,†,‡]

Chemistry Departments, University of Kansas, Lawrence, Kansas 66045, and The Ohio State University, Columbus, Ohio 43210

Received August 20, 1992

Studies are reported on the autoxidation, in the solvent system 3:1:1 acetone/pyridine/water (APW), of a series of iron(II) cyclidenes, of the general formula $[Fe(R^3,R^2,m\text{-xyl})Cl]^+$ with R^3 = Me, Ph and R^2 = Me, Bz, which have high relevance as dioxygen carrier model systems. Autoxidation rates can be modeled by an electron-transfer mechanism involving a parallel dioxygen adduct equilibrium, with the autoxidation reaction being driven by a subsequent reaction of the primary superoxide product. The deduced rate constants k' for the electron-transfer process decrease in the sequence MeMe > MeBz > PhMe > PhBz, which is the order of increasing electron-withdrawing power and/or steric bulk of the substituents. Products of the reaction were identified explicitly for one of the complexes (R^2 = R^3 = Me), employing mainly UV–vis and ESR spectroscopy. A remarkable product of the autoxidation of iron(II) cyclidenes in this specific solvent system, is a peroxoiron(III) species, which can even be observed at ambient temperatures. Its ESR properties (low-spin iron g = 2 signal with an extremely low anisotropy) are in close similarity to those of natural systems analogues, and in contrast to the first reported model systems. This species can be generated by five independent routes (autoxidation; $FeO_2 + e^-$; $Fe(II) + KO_2$; $Fe(III) + H_2O_2$; and $Fe(III) + C_6H_5IO$) in the basic medium, emphasizing its relevance both as a cytochrome P450 model and as example of O–O bond formation.

Introduction

Transition metal dioxygen carriers are of central importance to most respiring organisms and have attracted considerable study, especially the iron(II) porphyrin based hemoglobin and myoglobin found in the higher animals.[1] Considerable effort has been applied to replicate various aspects of the heme protein dioxygen carriers, not only to serve as models to better understand the natural systems, thereby augmenting the field of coordination chemistry, but also to study synthetic dioxygen carriers, which have an increasing significance in direct applications including O_2 purification and separation,[2] O_2 sensors, and, perhaps eventually, synthetic blood[3] and less direct applications including fuel cells/batteries, and catalysts for aerial oxidations of organic substrates.[4] There have been a number of excellent reviews on synthetic transition metal dioxygen carriers.[5] However, no dioxygen carrier has an unlimited in-service lifetime, and all O_2 carriers known to date suffer autoxidation (irreversible oxidation by O_2) in solution, including the biological systems. Typically 1.5–3% of the hemoglobin of human blood is oxidized to the iron(III) form, the so-called methemoglobin, each day.[6] However the actual concentration of methemoglobin is maintained below about 1% by an enzymic reduction process.[7] Autoxidation of dioxygen carriers is known to proceed via many types of mechanism, but despite many years of investigation, relatively few are understood in detail. Apparently, the autoxidation mechanism that occurs in any given case is dependent upon both the nature of the iron-(II) complex and experimental conditions. The works of Weiss,[8] George,[9] and Hammond,[10] and their associates on the autoxidation of hydrated ferrous ion and its complexes have provided a broadly accepted formulation for the bimolecular pathway to autoxidation of these species. Following the initial formation of the ferrous dioxygen complex, which may be formally considered to be $Fe^{III}(O_2^-)$, reaction with a second iron(II) yields a μ-peroxy-bridged iron(III) species. Homolytic cleavage of the O—O bond produces a ferryl species, (Fe=O), and then reaction of this iron-(IV) complex with another iron(II) species produces the thermodynamically stable μ-oxo dinuclear iron(III) product. Parallel studies by Caughey[11] and his co-workers on porphyrin complexes led to substantially the same bimolecular mechanism, and subsequently, elegant work by several groups has confirmed the proposed intermediates.[12]

Even though the μ-peroxo autoxidation mechanism has great generality, it cannot account for the autoxidation of the heme proteins, hemoglobin and myoglobin,[6,7] because each iron is isolated within a separate globular protein, thereby preventing μ-peroxo bridge formation. Further, the elucidation of the

[†] University of Kansas.
[‡] The Ohio State University.

(1) Antonini, E.; Brunori, M. In *Hemoglobin and Myoglobin in their Reactions with Ligands*; North-Holland Publishing Company: Amsterdam, 1971.
(2) (a) Norman, J. A. T.; Pez, G. P.; Roberts, D. A. In *Oxygen Complexes and Oxygen Activation by Transition Metals*; Martell, A. E., Sawyer, D. T., Eds.; Plenum Press: New York, 1988. (b) Stewart, R. F.; Estep, P. A.; Sebastian, J. J. S. *Bur. Mines Inf. Circ.* **1959**, 7906. (c) Adduci, A. J. *CHEMTECH* **1976**, 575.
(3) (a) Geyer, R. P. In *Erythrocyte Structure & Function*; Brewer, G. L., Ed.; Alan R Liss Inc.: New York, 1974. (b) Busch, D. H. *Critical Care Med.* **1982**, *10*, 246. (c) Bolin, R. B.; Geyer, R. P.; Nemo, G. J., Eds. *Advances in Blood Substitute Research*; Alan R. Liss, Inc.: New York, 1983.
(4) Busch, D. H. In *Oxygen Complexes and Oxygen Activation by Transition Metals*; Martell, A. E., Sawyer, D. T., Eds.; Plenum Publ. Corp.: New York, 1988.
(5) (a) Jones, R. D.; Summerville, D. A.; Basolo, F. *Chem. Rev.* **1976**, *19*, 1. (b) Niederhoffer, E. C.; Timmons, J. H.; Martell, A. E. *Chem. Rev.* **1984**, *84*, 137. (c) Traylor, T. G.; Traylor, P. S. *Annu. Rev. Biophys. Bioeng.* **1982**, *11*, 105. (d) Collman, J. P.; Halbert, T. R.; Suslick, K. S. In *Metal Ion Activation of Dioxygen*; Spiro, T. G., Ed.; John Wiley & Sons: New York, 1980; p 1. (e) Gubelmann, M. H.; Williams, A. F. In *Struct. Bonding* **1983**, *55*, 1. (f) Smith, T. D.; Pilbrow, J. R. *Coord. Chem. Rev.* **1981**, *39*, 295.
(6) (a) Eder, H. A.; Finch, C.; McKee, R. W. *J. Clin. Invest.* **1949**, *28*, 265. (b) Jaffe, E. R.; Neuman, G. *Nature* **1964**, *202*, 607.
(7) Bodansky, O. *Pharmacol. Rev.* **1951**, *3*, 144.
(8) Weiss, J. *Naturwissenschaften* **1935**, *23*, 64.
(9) George, P. *J. Chem. Soc.* **1954**, 4349.
(10) Hammond, G. S.; Wu, C. H. *Adv. Chem. Ser.* **1968**, *77*, 186.
(11) (a) Alben, J. O.; Fuchsman, W. H.; Beaudreau, C. A.; Caughey, W. S. *Biochemistry* **1968**, *7*, 624. (b) Cohen, I. A.; Caughey, W. S. *Biochemistry* **1968**, *7*, 636.
(12) (a) Chin, D. H.; Del Gaudio, J.; La Mar, G. N.; Balch, A. L. *J. Am. Chem. Soc.* **1977**, *99*, 5486. (b) Chin, D. H.; Balch, A. L.; La Mar, G. N. *J. Am. Chem. Soc.* **1980**, *102*, 1446. (c) Chin, D. H.; La Mar, G. N.; Balch, A. L. *J. Am. Chem. Soc.* **1980**, *102*, 4344.

0020-1669/93/1332-1086$04.00/0

μ-peroxo autoxidation mechanisms provided the spark that inspired Collman,[13] Baldwin,[14] Battersby,[15] and others to design sterically encumbered porphyrins in order to produce stable iron(II) dioxygen adducts. While the strategy succeeded, the improved ligand design did not completely eliminate autoxidation.[16] The autoxidation of Hb, Mb, and the hindered porphyrins implies that at least one additional autoxidation mechanism exists for dioxygen carriers. Studies on the autoxidation of hemoglobin and myoglobin have led to disagreement about the mechanism of that process, or processes, for the natural products. One school favors the bimolecular nucleophilic displacement of superoxide from the dioxygen adduct,[17] while the other attributes the autoxidation to an electron-transfer process between dioxygen and a six-coordinated iron(II) species.[18] Autoxidation of metal complexes by outer sphere electron transfer to dioxygen has been found for several transition metal complexes including various ruthenium ammines,[19] six-coordinate iron and osmium porphyrins, and iron(II) tris(4,7-dihydroxy-1,10-phenanthroline).[20]

Perhaps the most detrimental category of autoxidation processes for any transition metal complex is that of ligand oxidation,[21] since a metal-centered oxidation is expected to be relatively simple to reverse. Further details of the autoxidation of dioxygen carriers may be found in a recent review.[22]

Certain intermediates or products of the autoxidation, especially those containing reduced forms of dioxygen, are highly interesting, in view of the important field of dioxygen activation by such metalloenzymes as peroxidases and mono- and dioxygenases. The catalytic cycle of cytochrome P450, for example, features a low-spin iron(II) complex, which can reversibly bind oxygen (much like the oxygen carriers). Activation of the enzyme involves a second one-electron reduction by a cofactor, with the subsequent steps not being well understood. The postulated intermediates are a (peroxo)iron(III) complex, which yields the essential high-valent iron oxo species via O–O bond cleavage; the latter is believed to be the active oxidizing species,[23] although recent studies based on non-heme oxygenase model systems indicate the possibility of multiple catalytic pathways, implying that (hydroperoxo)iron(III) species per se might have catalytic activity.[24] Since 1978, several (peroxo)iron(III) model complexes have been discovered and are under investigation with the hope of further elucidating the activation mechanism.[25] However, only Tajima's model systems[26] show complete agreement with the characteristics (especially ESR) of the natural systems (P450, HRP, Mb, Hb, BLM).[27]

The cobalt(II) and iron(II) cyclidene complexes represent the most successful class of synthetic non-porphyrin dioxygen carrier. Reversible dioxygen binding has been achieved for both the cobalt and the iron complexes of some of these ligands.[28] The most notable of the iron(II) cyclidenes so far studied is $[Fe^{II}(Ph,Bz,m\text{-}xyl)]^{2+}$ (for notation, see structure I), which exhibits

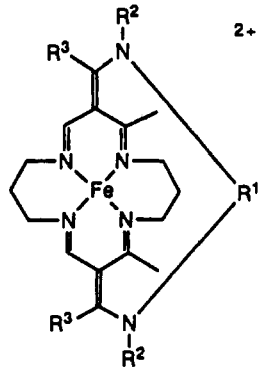

I

reversible dioxygen binding in aqueous 1-methylimidazole/acetone, with the remarkable autoxidation half-life of ~24 h at 20 °C.[29] However, most of the iron(II) cyclidenes are less stable in the presence of dioxygen and have autoxidation lifetimes which are considerably shorter. The wide range of autoxidative behavior of these iron(II) complexes provides a unique opportunity to investigate the fundamental chemistry of iron(II) dioxygen carrier autoxidation. These substances share the design features that forestall the previously described μ-peroxo bridge mechanism, and distinct advantages for the study of autoxidation derive from the extensive structural variation that is possible with these

(13) Collman, J. P.; Gagne, R. R.; Halbert, T. R.; Marchon, J. C.; Reed, C. A. *J. Am. Chem. Soc.* **1973**, *95*, 7868.
(14) Almog, J.; Baldwin, J. E.; Hugg, J. *J. Am. Chem. Soc.* **1975**, *97*, 227.
(15) Battersby, A. R.; Hamilton, A. D. *J. Chem. Soc., Chem. Commun.* **1980**, 117.
(16) Collman, J. P. *Accts. Chem. Res.* **1977**, *10*, 265.
(17) Shikama, K. *Coord. Chem. Rev.* **1988**, 73.
(18) (a) Wallace, W. J.; Houtchens, R. A.; Maxwell, J. C.; Caughey, W. S. *J. Biol. Chem.* **1982**, *257*, 4966. (b) Watkins, J. A.; Kawanishi, S.; Caughey, W. S. *Biochem. Biophys. Res. Commun.* **1985**, *132*, 742.
(19) Stanbury, D. M.; Haas, O.; Taube, H. *Inorg. Chem.* **1980**, *19*, 518.
(20) (a) Chu, M. M. L.; Castro, C. E.; Hathaway, G. M. *Biochemistry* **1978**, *17*, 481. (b) Billecke, J.; Kokisch, W.; Buchler, J. W. *J. Am. Chem. Soc.* **1980**, *102*, 3622. (c) Vu, D. T.; Stanbury, D. M. *Inorg. Chem.* **1987**, *26*, 1732.
(21) (a) Riley, D. P.; Busch, D. H. *Inorg. Chem.* **1983**, *22*, 4141. (b) Dabrowiak, J. C.; Busch, D. H. *Inorg. Chem.* **1975**, *14*, 1881. (c) Goedken, V. L. *J. Chem. Soc., Chem. Commun.* **1972**, 207.
(22) Warburton, P. R.; Busch, D. H. In *Perspectives in Bioinorganic Chemistry*; Hay, R. W., Ed.; Vol. 2, in press.
(23) (a) *Cytochrome P450: Structure, Mechanism, and Biochemistry*; Ortiz de Montellano, P. R., Ed.; Plenum: New York, 1986. (b) McMurry, T. J.; Grooves, J. T. In *Cytochrome P450: Structure, Mechanism, and Biochemistry*; Ortiz de Montellano, P. R., Ed.; Plenum: New York, 1986. (c) Gunter, M. J.; Turner, P. *Coord. Chem. Rev.* **1991**, *108*, 115. (d) Mansuy, D.; Battioni, P.; Battioni, J. P. *Eur. J. Biochem.* **1989**, *184*, 267.
(24) (a) Valentine, J. S.; Burstyn, J. N.; Margerum, L. D. In *Oxygen Complexes and Oxygen Activation by Transition Metals*; Martell, A. E., Sawyer, D. T., Eds.; Plenum Publ. Corp.: New York, 1988; p 175. (b) Yang, Y.; Diederich, F.; Valentine, J. S. *J. Am. Chem. Soc.* **1991**, *113*, 7195. (c) Nam, W.; Ho, R.; Valentine, J. S. *J. Am. Chem. Soc.* **1991**, *113*, 7052. (d) Wu, Y-D.; Houk, K. N.; Valentine, J. S.; Nam, W. *Inorg. Chem.* **1992**, *31*, 718.
(25) (a) Gubbelmann, M. H.; Williams, A. F. In *Transition Metal Complexes-Structures and Spectra*; Springer-Verlag: Berlin, Heidelberg, New York, Tokyo, 1983. (b) McCandlish, E.; Miksztal, A. R.; Nappa, M.; Sprenger, A. Q.; Valentine, J. S.; Stong, J. D.; Spiro, T. G. *J. Am. Chem. Soc.* **1980**, *102*, 4268. (c) Burstyn, J. N.; Roe, J. A.; Miksztal, A. R.; Shaevitz, B. A.; Lang, G.; Valentine, J. S. *J. Am. Chem. Soc.* **1988**, *110*, 1382. (d) Ahmad, S.; McCallum, J. D.; Shiemke, A. K.; Appelman, E. H.; Loehr, T. M.; Sanders-Loehr, J. *Inorg. Chem.* **1988**, *27*, 2230. (e) Fujii, S.; Ohya-Nishiguchi, H.; Hirota, N. *Inorg. Chim. Acta* **1990**, *175*, 27. (f) Tsang, P. K. S.; Sawyer, D. T. *Inorg. Chem.* **1990**, *29*, 2848. (g) Welborn, C. H.; Dolphin, D.; James, B. R. *J. Am. Chem. Soc.* **1981**, *103*, 2869. (h) Shirazi, A.; Goff, H. M. *J. Am. Chem. Soc.* **1982**, *104*, 6318.
(26) (a) Tajima, K. *Kagaku to Kogyo (Tokyo)* **1991**, *44*, 248. (b) Tajima, K. *Inorg. Chim. Acta* **1990**, *169*, 211. (c) Tajima, K. *Inorg. Chim. Acta* **1989**, *163*, 115. (d) Tajima, K.; Yoshino, M.; Mikami, K.; Edo, T.; Ishizu, K.; Ohya-Nishiguchi, H. *Inorg. Chim. Acta* **1990**, *172*, 83. (e) Tajima, K.; Shigematsu, M.; Jinno, J.; Ishizu, K.; Ohya-Nishiguchi, H. *J. Chem. Soc., Chem. Commun.* **1990**, 144. (f) Tajima, K.; Jinno, J.; Ishizu, K.; Sakurai, H.; Ohya-Nishiguchi, H. *Inorg. Chem.* **1989**, *28*, 709. (g) Tajima, K.; Shigematsu, M.; Jinno, J.; Kawano, Y.; Mikamo, K.; Ishizu, K.; Ohya-Nishiguchi, H. *Biochem. Biophys. Res. Commun.* **1990**, *166*, 924. (h) Tajima, K.; Shigematsu, M.; Jinno, J.; Ishizu, K.; Ohya-Nishiguchi, H. *Stud. Surf. Sci. Catal.* **1991**, *66*, 305.
(27) (a) Stubbe, J.; Kozarich, J. W. *Chem. Rev.* **1987**, *87*, 1107. (b) Symons, M. C. R.; Petersen, R. L. *Biochim. Biophys. Acta* **1978**, *535*, 241. (c) Bartlett, N.; Symons, M. C. R. *Biochim. Biophys. Acta* **1982**, *744*, 110. (d) Gasyna, Z. *FEBS Lett.* **1979**, *106*, 213. (e) Kappl, R.; Hohn-Berlage, M.; Huettermann, J.; Bartlett, N.; Symons, M. C. R. *Biochim. Biophys. Acta* **1985**, *827*, 327. (f) Davydov, R.; Kappl, R.; Huetterman, J.; Peterson, J. A. *FEBS Lett.* **1991**, *295*, 113.
(28) (a) Stevens, J. C.; Busch, D. H. *J. Am. Chem. Soc.* **1980**, *102*, 3285. (b) Herron, N.; Busch, D. H. *J. Am. Chem. Soc.* **1981**, *103*, 1236. (c) Herron, N.; Zimmer, L. L.; Grzybowski, J. J.; Olszanski, D. J.; Jackels, S. C.; Callahan, R. W.; Cameron, J. H.; Christoph, G. G.; Busch, D. H. *J. Am. Chem. Soc.* **1983**, *105*, 6585. (d) Busch, D. H. *Trasfus. Sangue* **1988**, *33*, 57. (e) Busch, D. H. In *Oxygen Complexes and Oxygen Activation by Transition Metals*; Martell, A. E., Sawyer, D. T., Eds.; Plenum Publ. Corp.: New York, 1988.
(29) Herron, N.; Cameron, J. H.; Neer, G. L.; Busch, D. H. *J. Am. Chem. Soc.* **1983**, *105*, 298.

complexes (largely through alterations in the bridging group R^1 and the groups flanking the cavity entrances, R^2 and R^3). Of greatest importance, the dioxygen affinity and the susceptibility toward autoxidation vary with these substituents. As a result it is possible to select species ideally suited to investigate certain aspects of the autoxidation reaction. The first lacunar dioxygen carrier reported, R^1 = *m*-xylylene and $R^2 = R^3 = CH_3$, has been ideal for these studies because it undergoes autoxidation in a temperature range low enough to permit study of important reactive intermediates.

Experimental Section

Materials. Solvents and reagents were reagent grade or better. Solvents were distilled under nitrogen and degassed (freeze–pump–thaw method) prior to use. The synthetic route to the iron(II)[28c] and iron(III)[30] complexes has been described previously.

Physical Measurements. ESR spectra were recorded on a Varian E-112 spectrometer operating in the X-band and the magnetic field was calibrated with external DPPH (g = 2.0036). Cyclic voltammetry experiments were performed using a Princeton Applied Research potentiostat (Model 173) and universal programmer (Model 175), the output being recorded directly to paper using a Houston Instruments 200 chart recorder. The working electrode was a 3-mm-diameter vitreous carbon disk, sealed into Kel F (Bioanalytical Systems Inc.), the secondary/counter electrode was a platinum wire of large surface area, and the reference electrode was a silver wire. All electrode potentials were measured vs. ferrocene, which was used as an internal standard. The supporting electrolyte was 0.05 M LiCl. UV–visible spectrophotometric studies were conducted using a 1-cm gastight quartz cell, fitted with a gas inlet and a bubbling tube. Spectra were recorded on either a Varian 2300 spectrophotometer or a Hewlett-Packard 8452 diode array spectrophotometer, with a Model 9000 (300) Hewlett-Packard Chem Station. Both instruments incorporated flow-through temperature regulated cell holders connected to a Neslab constant temperature circulation system, giving a temperature precision of ±0.3 °C. Oxygen/nitrogen gas mixtures were generated using Tylan FC-260 mass flow controllers. All inert-atmosphere manipulations were performed in a nitrogen filled Vacuum Atmospheres Corp. (VAC) glovebox, equipped with a gas circulation and oxygen removal system—either a VAC MO40-1 or HE-493 dry train. Oxygen concentrations were maintained below 1 ppm. Typical kinetic experiments involved filling a 1-cm gastight cell, fitted with a gas inlet and a bubbling tube, inside the glovebox with a solution of ca. 2×10^{-4} M of the cyclidene complex in APW. Solutions were saturated by initial bubbling for 120–180 s with the desired gas mixtures. Pseudo-first-order conditions of constant oxygen concentrations were achieved by occasionally bubbling more O_2 into the solution during the course of the experiment. Kinetic studies were performed on either of the above spectrophotometers, and the kinetic parameters were evaluated using either the Hewlett-Packard proprietary software or programs written in Basic for the Varian spectrophotometer by Dr. Naidong Ye of this group.

Results and Discussion

Autoxidation of [Fe^{II}(Me,Me,*m*-xyl)Cl]$^+$ in Acetone–Pyridine–Water. In a solvent consisting of 3:1:1 by volume acetone–pyridine–water (311APW, apparent pH ca. 10) the five-coordinate iron(II) complex [Fe^{II}(Me,Me,m-xyl)Cl]$^+$ is a fully reversible dioxygen carrier at –41 °C with a P_{50} of about 6 Torr. However, at temperatures above –35 °C, an irreversible autoxidation process becomes competitive with the reversible dioxygen binding reaction.[28b,c,29] A particular benefit that derives from this low temperature (–35 °C) autoxidation is the opportunity to observe the formation of the initial products of the primary redox event and that opportunity has been exploited in this work.

The autoxidation of [Fe(Me,Me,m-xyl)Cl]$^+$ has been studied by UV-Vis and ESR spectroscopy. (1) Rate data on the autoxidation reaction have been compared with rate laws predicted for idealized mechanisms; (2) the spectral properties of the initial products of the primary redox events have been sought and used in further mechanistic interpretations; (3) given the proposed structures of these intermediates, they have then been generated by other logical routes.

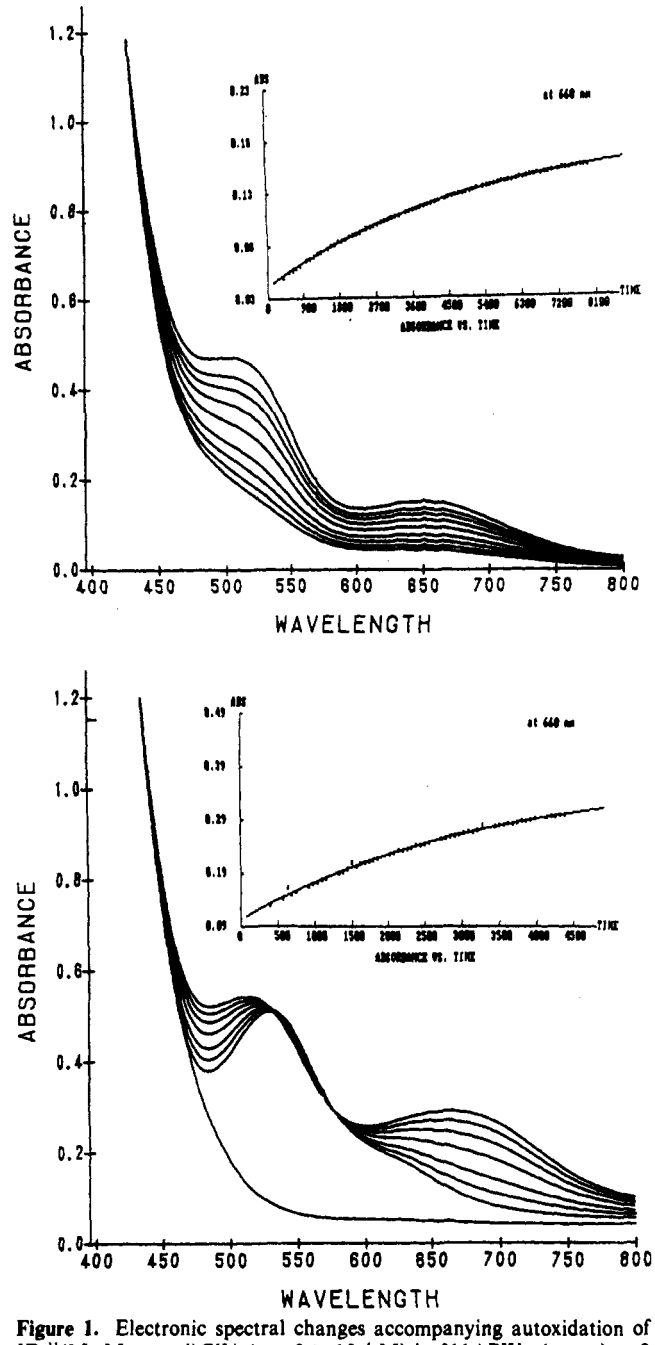

Figure 1. Electronic spectral changes accompanying autoxidation of [Fe^{II}(Me,Me,*m*-xyl)Cl]$^+$ ($c = 2 \times 10^{-4}$ M) in 311APW: (a, top) at 0 °C, 12 Torr; (b, bottom) at –20 °C, 760 Torr. Inserts show the kinetic traces at 660 nm and the first-order fits (solid lines).

The product distribution and, therefore, the spectral changes accompanying the reaction depend on the oxygen pressure used. Parts a and b of Figure 1 illustrate the UV–vis spectral changes on autoxidation of solutions equilibrated with 12 and 760 Torr of dioxygen, respectively. The smaller insets in these figures show the first-order kinetic behavior of the reaction, as determined at 660 nm. The solid line in the latter is calculated, and the symbols represent experimental points. At high dioxygen pressures, low temperatures and an opportune ratio of concentrations of dioxygen to iron complex, one can observe the conversion of the initially formed dioxygen adduct (λ_{max} 523, 619 sh nm[28b]) into products (λ_{max} ca. 500, 670 nm sh), Figure 1b. The set of spectra show three clean isosbestic points at 438, 530, and 574 nm. At low dioxygen pressures (Figure 1a), the spectra show the formation of a product with maxima at 500 and 650 nm (sh) with now only one isosbestic point around 440 nm and give no indication

(30) Padolik, P. A. Ph.D. Thesis, The Ohio State University, 1989.

Table I. Comparison of Autoxidation Rates of Fe–Cyclidenes (R^1 = mxyl) in APW

complex	T, °C	solvent/salt	P_{O_2}, torr	k_{obs}, s^{-1}	comments
MeMemxyl	−20	APW	37.4	1.23×10^{-4}	
			70.4	1.72×10^{-4}	
			97.5	1.98×10^{-4}	
			295.4	2.44×10^{-4}	
			748.4	2.82×10^{-4}	
	−20	APW/$NaNO_3$ 0.05M	12.7	8.8×10^{-5}	
			38	2.0×10^{-4}	
			102	2.7×10^{-4}	
			204.5	3.5×10^{-4}	
			380	3.3×10^{-4}	
			760	3.3×10^{-4}	
	−23	APW	12.5	1.2×10^{-4}	
			25	1.6×10^{-4}	
			102	2.6×10^{-4}	
			202	4.2×10^{-4}	
			760	4.4×10^{-4}	
	0	APW	12.7	1.86×10^{-4}	
			38	4.42×10^{-4}	
			154	1.45×10^{-3}	
			380	2.20×10^{-3}	
	0	APW	(760	1.9×10^{-3})	
	12	APW	760	7.2×10^{-3}	pH 9.78
			760	5.9×10^{-3}	pH 9.72, added HCl
			760	3.9×10^{-3}	pH 9.33
			760	4.0×10^{-3}	pH 9.03
			760	2.5×10^{-3}	pH 8.29
	25	APW	19	3.15×10^{-4}	all $+2 \times 10^{-4}$ M HCl
			38	6.28×10^{-4}	
			76	9.53×10^{-4}	
			152	1.75×10^{-3}	
			304	3.60×10^{-3}	
			760	8.67×10^{-3}	
MeBzmxyl	0	APW	38	7.0×10^{-5}	
			150	2.5×10^{-4}	
			300	3.9×10^{-4}	
			760	6.7×10^{-4}	
	12	APW	760	2.26×10^{-3}	pH 9.78
			760	1.69×10^{-3}	pH 9.69, added HCl
			760	1.20×10^{-3}	pH 9.30
			760	0.52×10^{-3}	pH 8.99
			760	0.38×10^{-3}	pH 8.30
			760	0.46×10^{-3}	pH 8.00
	25	APW	19	7.4×10^{-5}	all $+2 \times 10^{-4}$ M HCl
			38	1.55×10^{-4}	
			101	2.4×10^{-4}	
			202	6.0×10^{-4}	
			380	8.6×10^{-4}	
			760	1.7×10^{-3}	
PhMemxyl	0	APW	(760	4.2×10^{-4})	
	20	APW	760	1.6×10^{-2}	pH 9.78
			760	1.0×10^{-2}	pH 9.75, added HCl
			760	1.21×10^{-3}	pH 9.69
			760	3.55×10^{-4}	pH 9.30
			760	2.25×10^{-4}	pH 8.99
			760	1.9×10^{-4}	pH 8.69
			760	1.6×10^{-4}	pH 8.30
	25	APW	19	2.05×10^{-5}	all $+2 \times 10^{-4}$ M HCl
			38	3.7×10^{-5}	
			101	5.0×10^{-5}	
			202	1.41×10^{-4}	
			380	2.35×10^{-4}	
			760	5.25×10^{-4}	
PhBzmxyl	0	APW	(760	8×10^{-5})	
	20	APW	760	6.0×10^{-3}	pH 9.78
			760	5.1×10^{-3}	pH 9.76, added HCl
			760	6.2×10^{-4}	pH 9.37
			760	2.3×10^{-4}	pH 9.07
			760	1.05×10^{-4}	pH 8.76
			760	1.65×10^{-4}	pH 8.38
			760	2.15×10^{-4}	pH 8.08
	25	APW	19	1.85×10^{-5}	all $+2 \times 10^{-4}$ M HCl
			38	4.7×10^{-5}	
			101	6.5×10^{-5}	
			202	1.3×10^{-4}	
			380	1.7×10^{-4}	
			760	3.3×10^{-4}	

of the presence of a dioxygen adduct during the reaction. Kinetic data approximate the first-order rate law for low and high dioxygen pressures for at least three half-lives but deviate slightly for intermediate pressures, being a little faster in the beginning. Further, for the latter cases, the observed rate constants measured at different wavelengths (e.g., 510 and 650 nm) can vary by 10–30%, with the rate constant at 510 nm usually being the greater for unbuffered systems. This is probably due to presence of a third chromophore, which is also manifested by the shift of the long wavelength maximum (650–670 nm) going from low to high dioxygen pressures. Such a change is to be expected because of the appearance of dioxygen adduct as the dioxygen partial pressure increases. The resulting discrepancies are small enough to warrant the conclusion that the choice of observation wavelength is not critical.

Table I summarizes the pseudo-first-order rate constants for a variety of conditions. Figure 2 reports the dioxygen dependence of the rates of product formation (measured at 650 nm and for −20 °C). The reaction rate increases linearly with dioxygen pressure at low pressures but reaches a saturation value at high pressures. Saturation behavior typically emanates from either preequilibrium or competitive equilibrium reactions. In the most obvious model, preequilibrium formation of the dioxygen adduct precedes superoxide dissociation as shown in eqs 1 and 2, giving

$$Fe^{II} + O_2 \rightleftharpoons Fe(O_2) \quad K_{O_2} \tag{1}$$

$$Fe(O_2) \rightarrow Fe^{III} + O_2^- \quad k \tag{2}$$

the rate law in eq 3. However, a rate law of precisely the same

$$\text{rate} = kK_{O_2}[Fe^{II}][O_2]/(1 + K_{O_2}[O_2]) \tag{3}$$

algebraic form describes a process involving a competitive equilibrium, in which dioxygen binding competes with electron transfer (eqs 4 and 5). The rate law is shown in eq 6. Both

$$Fe^{II} + O_2 \rightleftharpoons Fe(O_2) \quad K_{O_2} \tag{4}$$

$$Fe^{II} + O_2 \rightarrow Fe^{III} + O_2^- \quad k' \tag{5}$$

$$\text{rate} = k'[Fe^{II}][O_2]/(1 + K_{O_2}[O_2]) \tag{6}$$

mechanisms predict saturation kinetics with zero order dependence of the rate on $[O_2]$ at high $[O_2]$, and first-order dependence at low concentrations. The double reciprocal plot ($1/k_{obs}$ vs. $1/p_{O_2}$)

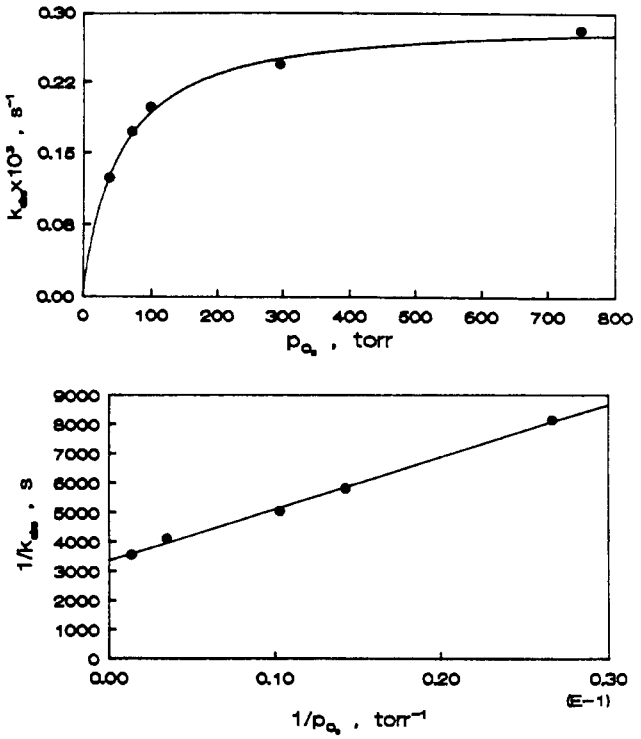

Figure 2. Dioxygen partial pressure dependence on the rate of autoxidation and double reciprocal plot for $[Fe^{II}(Me,Me,m\text{-xyl})Cl]^+$ in 311APW at −20 °C.

Table II. Comparison of Kinetic Parameters of Fe–Cyclidenes (R^1 = mxyl) in APW

complex	T, °C	solvent/ salt	K_{O_2}, torr^{-1}	k', torr^{-1} s^{-1}	extrapolated[28c,29] K_{O_2}, torr^{-1}
MeMemxyl	−20	APW	0.019	5.6×10^6	0.020
	−20	APW/ $NaNO_3$ 0.05M	0.022	8.9×10^6	0.020
	−23	APW	0.032	1.3×10^5 (650nm)	0.026
			0.039	2.0×10^5 (510nm)	
	0	APW	0.0055	1.6×10^5	0.0039
	0	APW	0.0031	9.9×10^6	0.0039
	25	APW		1.1×10^5 [a]	0.00068
MeBzmxyl	0	APW	0.0016	2.0×10^6	0.00041
	25	APW		2.2×10^6 [a]	0.000052
PhMemxyl	0	APW	0.0018	6.5×10^7	0.0013
	25	APW		6.8×10^7 [a]	0.00015
PhBzmxyl	0	APW	0.0025	1.7×10^7	0.0026
	25	APW		4.0×10^7 [a]	0.00016

[a] From slope k_{obs} vs p.

of Figure 2 confirms this behavior and yields kinetic parameters. Because available evidence favors the competitive equilibrium/electron-transfer mechanism (hence forward CEET mechanism),[22,28d,31] Table II reports the parameters k'(=1/slope) and K_{O_2} (=intercept/slope). The solid line drawn in Figure 2 is calculated on the basis of the derived kinetic parameters and eq 6. The calculated K_{O_2} values agree well with those extrapolated from equilibrium measurements.[29,28c]

The Primary Reaction Products. Electron spin resonance experiments have led to identification of the initial reaction products arising from the primary electron transfer event. Figure 3 shows typical ESR spectral changes that have been observed during autoxidation. Solutions were oxygenated at temperatures in the range from −50 to −60 °C and ESR spectra were measured at liquid nitrogen temperatures on solutions that had been annealed at ca. 0 °C or room temperature for various time periods. It should be noted here, that in order to justify comparison of UV–vis and ESR spectral changes, minimal concentrations of the iron cyclidene complex were used, but available ESR equipment still made it necessary to use concentrations for ESR experiments that exceeded those used in UV–vis studies by a factor of 10. Furthermore, even with that higher concentration, the quality of the ESR spectra was compromised (signal/noise, baseline); however, the spectra were adequate for the necessary interpretations. The ESR investigations confirm the suspected complexity of the system, as indicated earlier by the UV–vis kinetic measurements. Depending on the reaction conditions, from one to four different paramagnetic products were observed. The resonance pattern in the vicinity of $g = 6$ (6.4, 5.8), which arises from the familiar high-spin iron(III) cyclidene complex, is present under all conditions and identifies the only product formed at low dioxygen pressures. That species probably has a five- or six-coordinate structure in which the axial pyridine is replaced by hydroxide, because a very similar spectral pattern can be obtained in solvent systems composed of acetone–base–water, where pyridine is replaced by the noncoordinating bases collidine or lutidine, and in a MeOH–LiCl system.[31c] A six-coordinate structure cannot be ruled out, since the signal has the rather broad characteristics of six-coordinate high-spin iron(III) complexes, in which weak ligands bind to both axial positions.[26c,32] This spectrum can also be produced by chemical or electrochemical oxidation of the iron(II) cyclidene complex.

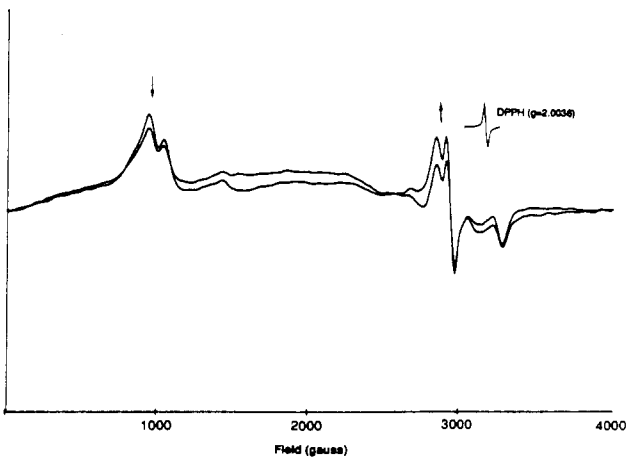

Figure 3. ESR spectra of a frozen (−196 °C) solution of $[Fe^{II}(Me,Me,m\text{-xyl})Cl]^+$ ($c = 3 \times 10^{-3}$ M) in 311APW during autoxidation at 760 Torr of O_2, annealed at room temperature for 1 and 2 min.

A quickly formed spectral pattern near $g = 2$, having highly distinctive spectral parameters, appears with O_2 pressures above ca. 20 Torr but is not observed at lower dioxygen pressures. The resonances display an exceptionally weak orthorhombic anisotropy (g values of 1.93, 2.16, and 2.23) and indicate the presence of a low-spin, six-coordinate, rhombic iron(III) complex. After longer periods of autoxidation and especially noticeable at higher O_2 pressures, a second, overlapping spectrum occurs in the region near $g = 2$ with a similar array of g values (1.97, 2.10, 2.25). In addition to these signals, especially on longer autoxidation time scales at higher O_2 pressures, a weak, relatively narrow absorption is found near $g = 4.3$, which has been attributed to rhombic, six-coordinate, high-spin iron(III). On the basis of its position and line shape, that final spectrum is believed to be indicative of a product that does not contain a tetraazamacrocycle but rather contains some simpler chelating ligand, possibly formed via ring

(31) (a) Herron, N.; Chavan, M. Y.; Busch, D. H. *J. Chem. Soc., Dalton Trans.* **1984**, 1491. (b) Herron, N.; Dickerson, L.; Busch, D. H. *J. Chem. Soc., Chem. Commun.* **1983**, 884. (c) Sauer-Masarwa, A.; Dickerson, L.; Herron, N.; Busch, D. H. *Coord. Chem. Res.*, in press. (d) Dickerson, L.; Sauer-Masarwa, A.; Herron, N.; Fendrick, C.; Busch, D. H. *J. Am. Chem. Soc.*, in press.

(32) Ohtsuka, T.; Ohya, T.; Sato, M. *Inorg. Chem.* **1985**, *24*, 776.

Table III. ESR Data for Natural Systems and Model Hydrogen Peroxide Complexes

complexes	method of preparation	solvent	T^a	g_1	g_2	g_3	ref
Fe^{III}MeMemxyl–OOH	autoxidation of Fe^{II} or Fe^{III} + H_2O_2 or $FeO_2 + e^-$	APW	0 °C	1.93	2.16	2.23	this work
				1.97	2.10	2.25	this work
Fe^{III}MeMemxyl–OOH	autoxidation of Fe^{II} or Fe^{I} + KO_2 or $FeO_2 + e^-$	CH_3CN/MIM	0 °C	1.93	2.13	2.21	this work
				1.98	2.11	2.24	this work
reduced oxyferrous $P450_{cam}$	X-irradiation of $P450_{cam}$:substrate:O_2	H_2O	77 K	1.95	2.17	2.27	27f
Fe^{III}Hb–OOH	UV or γ-irradiation of FeO_2	H_2O	77 K	1.967	2.148	2.265	27e
Fe^{III}Mb–OOH	UV or γ-irradiation of FeO_2 also powder	H_2O	77 K	1.941	2.176	2.296	27e
		H_2O	77 K	1.97	2.11	2.21	27d,b
		H_2O	120–160 K	1.94	2.16	2.30	27d
Fe^{III}HRP–OOH	γ-irradiation of oxyHRP	H_2O	120–160 K	1.95	2.16	2.31	27d
Fe^{III}BLM–OOH	Fe^{III}BLM + H_2O_2 or $FeO_2 + e^-$	H_2O		1.94	2.17	2.25	27a
Fe^{III}OEP(OH)–OOH	FeO_2 + AscNa	DMF/H_2O	–40 °C/77 K[b]	1.953	2.171	2.286	26e,h
	$Fe^{III} + H_2O_2$	DMF/H_2O	–45 °C/77 K[b]	1.955	2.171	2.287	26e,h
Fe^{III}TPP(OH)–OOH	$Fe^{III} + H_2O_2$ with KOH base	DMF/H_2O	–45 °C/77 K[b]	1.961	2.159	2.266	26c
	$Fe^{III} + H_2O_2$ with TPA base	DMF/H_2O	–45 °C/77 K[b]	1.962	2.157	2.264	26c
Fe^{III}OEP–OOH	$FeO_2 + e^-$, $Fe^{II} + O_2^-$, $Fe^{I} + O_2$	CH_3CN/DMSO (1:1)	–25 °C	high spin 4.2[sharp], 2[weak]			25g
Fe^{III}OEP–OOH	$Fe^{II} + O_2^-$	CH_3CN or DMSO	room temp	high spin 4.2 (1.3, 9.5)			25b
Fe^{III}TPP–OOH	$Fe^{II} + O_2^-$	CH_3CN or DMSO	room temp	high spin 4.2 (1.3, 9.5)			25b
Fe^{III}EDTA–OOH	$Fe^{III} + H_2O_2$, pH 7.6	H_2O		3.90	4.15	4.39	25e
	$Fe^{III} + H_2O_2$, pH 11.2	H_2O		3.37	3.81	5.08	25e

[a] Reaction or annealing temperature, all ESR spectra recorded at 77 K. [b] Rapid mixing and freezing (within seconds).

opening.[26c,e] In aprotic solutions of porphyrins, a g value around $g = 4.3$ has also been attributed to a bidentate (peroxo)iron(III) species.[25b,c,g] In contrast, studies on FeEDTA show, that, depending on the pH of the solution, the addition of H_2O_2 leads to signals with more or less rhombic distortions, which have been attributed to peroxo species, possibly involving end-on, side-on equilibria. These spectra were easily distinguished from the sharp, narrow signal of the Fe^{III}EDTA itself in basic solutions.[25e] We cannot rule out the possibility that the $g = 4.3$ in our system reflects the eventual formation of a side-on peroxo complex, but it is difficult to imagine why the equilibrium shifts toward this species from the end-on form (vide infra) only at very long times on the autoxidation time scale in the basic solvent APW. On that time scale, it seems rather more likely that the peroxide has been destroyed.

The nature of the low-spin iron(III) complex (ESR signal near $g = 2$) is very important to the understanding of the fundamental mechanistic processes. Clearly this intermediate is an iron complex that has incorporated a sixth, relatively strong ligand in order to change to the low-spin state. That sixth ligand is almost certainly derived from dioxygen because the separately characterized Fe^{III} complex fails to produce such a spectrum when dissolved in the same solvent system.

The extremely small anisotropy displayed by the g values of this complex provides the essential information to identify the sixth ligand. This is a very characteristic feature of low-spin (peroxo)iron(III) complexes, especially those prepared from complexes of macrocyclic ligands in alkaline media.[26] Table III compares ESR parameters for iron peroxide complexes derived from natural systems and model complexes of macrocyclic ligands and EDTA. It is particularly interesting that the earliest known examples of (peroxo)iron(III) complexes seemed to militate against this formulation for the species described here. Until 1975, no (peroxo)iron(III) species were known[33] and the complexes of this class first reported[25] were high-spin iron(III) species, showing ESR signals at about $g = 4.3$, in contrast to the systems reported here, a number of natural systems, and their models.

Gasyna[27d] and Symons and Petersen,[27b] independently, were the first to identify low-spin mononuclear (peroxo)iron(III) complexes in studies with the natural systems myoglobin and HRP. Subsequently, Tajima et al. prepared two low-spin hydrogen peroxide complexes of iron(III) by the reaction of iron(III) porphyrins (TPP or OEP) with H_2O_2 and by the reduction of a dioxygen adduct of an iron(III) porphyrin with ascorbic acid. Both reactions were carried out under alkaline conditions and a rapid mixing and freezing technique was employed, because the (peroxo)iron(III) complexes decomposed rapidly, even at –45 °C. It was suggested that the decomposition involved opening of the porphyrin ring to form a tetrapyrrole chain, since the authors believed that the ESR signal around $g = 4.3$ implied the formation of a high-spin non-heme iron complex.[26c,e,h] Tajima suggests OH^- as the second axial ligand for his iron(III)–hydrogen peroxide–porphyrin complexes, even though the iron porphyrin–dioxygen adducts were originally coordinated to pyridine. In the case of Tajima's (alkylperoxo)iron(III) porphyrin complexes, the occurrence of two sets of ESR signals near $g = 2$ was explained by assuming the coordination of one or two alkylperoxide ligands.

As Table III shows, low-spin iron(III)–hydrogen peroxide complexes with anomalously small g anisotropies have also been reported for a variety of natural systems. These include an activated form of bleomycin, which can be prepared by one-electron reduction of the dioxygen adduct, [Fe(BLM)(O_2)], or reaction of [Fe^{III}(BLM)] with H_2O_2,[27a] and the peroxo iron complexes of hemoglobin, myoglobin, and horseradish peroxidase that have been prepared by one-electron reduction of the respective dioxygen adducts using pulse radiolysis or by UV radiation.[27b–e] The occurrence of a second, very similar resonance pattern in the $g = 2$ region was attributed to protonation of the primary reduced species. Also, recently the ESR spectrum of "reduced oxyferrous-P450cam" was reported, featuring again a $g = 2$ signal with rhombic symmetry and very small g anisotropy.[27f]

If the low-spin autoxidation products of [Fe(Me,Me,*m*-xyl)Cl]$^+$ do indeed contain the (peroxo)iron(III) unit, then this species should be accessible by other reactions, as indicated above, and solutions of the species in question have been prepared by four such techniques.

(1) Under conditions where the dioxygen adduct is stable (–40 °C in 311APW), the addition of 1 equiv of ascorbic acid to the oxygenated solution does indeed generate a solution whose frozen ESR signal is entirely low spin, with no high-spin signal whatsoever.

(2) The addition of 1 equiv of hydrogen peroxide to the high-

(33) Vaska, L. *Acc. Chem. Res.* **1976**, *9*, 177.

spin, five-coordinate iron(III) complex produces the familiar low-spin ESR spectrum, but in this case with (again) the second low spin rhombic signal of lesser intensity superimposed on it. The relative intensities of these two signals depend markedly on the details of the reaction procedure. If the reaction is carefully kept cooled to −20 °C during mixing of the iron complex and the H_2O_2, then the second signal is almost absent, but if the mixing is done at room temperature, followed by immediate freezing to −196 °C, then the second signal is about 50% as intense as the first one. Excess H_2O_2 also tends to increase the second signal.

(3) The reaction between the iron(II) cyclidene complex and superoxide failed to give the desired product in the APW solvent system; however, the proposed (peroxo)iron(III) complex was evidenced by experiments in acetonitrile. The injection of less than 1 equiv of KO_2 (from 5×10^{-2} M solution in DMSO/dibenzo-18-crown-6) into a solution of the Fe^{II} complex in acetonitrile–1.5 M *N*-methylimidazole, kept carefully cooled to −30 °C, produces low-spin species with characteristic ESR parameters similar to those observed in the APW solvent system (see Table III). The $g = 2$ product dominates and only traces of the second $g = 2$ signal grow in with additional KO_2 injections. Also concomitantly with the appearance of the signals in the $g = 2$ region is a rather large $g = 4.4$ signal, indicating decomposition of the cyclidene under the experimental conditions. Decomposition of the cyclidene ligand is not unlikely under highly basic aprotic conditions. The peroxo group produced in the superoxide reaction is highly basic and could deprotonate the R^3 methyl group (structure I), a process that has been linked to autoxidation.[34] We have also shown that in very dry acetonitrile–pyridine the reaction with superoxide produces a different species, characterized by an axial ESR signal (g = 2.16, 1.97). This species, which is also a product of the autoxidation in that solvent, probably contains peroxo groups with the lowest degree of protonation that has been observed for end-on bound peroxide in macrocyclic iron(II) complexes.

(4) Finally, an unexpected source of the same species was discovered which, in retrospect, is entirely understandable. In attempts to generate hypervalent Fe=O species with the cyclidene complexes and using iodosobenzene and $NaIO_4$, it was discovered that the two previously observed low-spin species could be generated; however, the formation of those species depended on the availability of water and the presence of a strong axial ligand such as pyridine or *N*-methylimidazole. Using [Fe(Me,Me,*m*-xyl)Cl]$^+$ in 311APW, the addition of PhIO or $NaIO_4$ produced ESR spectra identical to those of the superimposed pair of low-spin species observed in the reactions of the iron complex with H_2O_2. Iodosobenzene is much more efficient at producing these low-spin signals than is $NaIO_4$. Experiments under anhydrous conditions have been especially illuminating. When the reaction between PhIO and [Fe(Me,Me,*m*-xyl)Cl]$^+$ was carried out in anhydrous 3:1:1 acetone–pyridine–methanol, *no low-spin signal was generated*. Equally important, when a few drops of water were added to the solution, the low spin spectra appeared. The rational conclusion is summarized in eq 7, which avoids the

$$Fe^{III} + PhIO + H_2O \Leftrightarrow Fe^{III}(O_2^{2-}) + PhI \qquad (7)$$

question of whether an Fe=O intermediate is involved. The extent of protonation of the (peroxo)iron(III) complex is also not addressed. The implication that the O–O bond of peroxide has been formed under the influence of the iron atom deserves further investigation. Recently there has been mounting evidence that, at least for non-heme iron systems, the high-valent iron oxo species might not necessarily be the active oxidizing species in oxidase and oxygenase model systems. In the case of heme-containing systems, it is believed that the activation barrier for O–O bond cleavage can be lowered by the complexation of the resulting oxygen atom to the iron porphyrin center. In the case of the non-heme systems, however, comparable high-valent metal oxo species have not been characterized; instead, the {(hydro)peroxo}iron complexes, *N*-oxide complexes, or I^{III} species (in the systems based on Fe^{III} and iodosobenzene) are indicated to be possible sources of the catalytic activity. Therefore the possibility of multiple reaction pathways has been postulated.[24] The experimental results for this non-porphyrin–iron system provide further support for those findings. The (peroxo)iron species of this study are not only stable under ambient conditions, but they are also formed as products of the reaction of iodosobenzene with iron(III), with no evidence for the intermediate formation of high-valent iron oxo species. Clearly, investigations into the catalytic activity of the (peroxo)iron species, including oxygen activation, should be intensified, with special emphasis on systems were the (peroxo)iron intermediate is validated. It has been established, that iron(III) cyclidenes catalyze monooxygenation of small organic substrates in acetonitrile, with iodosobenzene. Higher turnovers were observed with the cyclidenes having smaller cavity sizes, so that it was concluded that oxidations mainly take place at the side opposite the cavity.[35,30] Unfortunately no oxidation products but fast destruction of the catalyst was experienced in aqueous acetonitrile with iron(III) cyclidenes–iodosobenzene in oxidation studies on vinylpyridines, which were also expected to bind in the axial side,[30] a system which is similar to the APW system described here. Oxidations of toluene in water with hydrogen peroxide and a series of cyclidenes demonstrated, that selective oxidations can be effected. The ratio of oxidation products cresols to benzaldehyde was dependent on the cavity size of the macrocycle. The data strongly suggest, that at least some of the oxidations are occurring inside the cavity in the complexes with more commodious voids. Unfortunately, again, the yields were quite low due to rapid destruction of the catalyst under the reaction conditions.[35]

The total consistency of this extensive chemistry, employing five routes to the same peroxoiron(III) species, certainly establishes the general nature of the intermediates in the autoxidation process.

The existence of two low-spin species remains somewhat troublesome. Three possible sources of this duality of substances are apparent: the peroxo ligand might be, as Gasyna has assumed in other systems, protonated to different degrees in the two substances; a simple possibility is the presence of different axial ligands trans to the peroxo ligand;[36] finally, for lacunar cyclidenes but not for simple porphyrins, the peroxo ligand might be inside the cavity in one case and outside the cavity in the other. The possibility that different axial ligands cause the duality of spectra was investigated by repeating the PhIO–3:1:1 APW experiments in a variety of solvent systems of the compositions 3:1:1 acetone–base–water, where the base was, in turn, pyridine, 2,6-lutidine, 2,4,6-collidine, and 1-methylimidazole. Superimposed spectra for two low-spin species were observed in all cases, even with bases that cannot coordinate in the axial site (2,6-lutidine and 2,4,6-collidine). The spectra for the noncoordinating bases, however, show much larger splitting of their g values, indicating axial ligands other than peroxide. However, only the ESR spectra associated with the two noncoordinating bases were identical; the superimposed pairs of rhombic signals from solvent system to solvent system otherwise showed no common species. Axial ligands appear to be implicated, but they do not account for the duality of signals.

It has been shown that the μ-oxo-dinuclear complex is an eventual product of autoxidation in aqueous solutions[30] and in MeOH/LiCl,[31c] even with lacunar cyclidenes. Also, the hydroxo

(34) (a) Goldsby, K. A.; Jircitano, A. J.; Nosco, D. L.; Stevens, J. C.; Busch, D. H. *Inorg. Chem.* **1990**, *29*, 2523. (b) Masarwa, M.; Warburton, P. R.; Evans, W. E.; Busch, D. H. Manuscript in preparation.

(35) Coltrain, B. K. Ph.D. Thesis, The Ohio State University, 1984.

(36) Tajima assumed hydroxide to be the axial ligand even though he started with pyridine as the axial ligand.[31c]

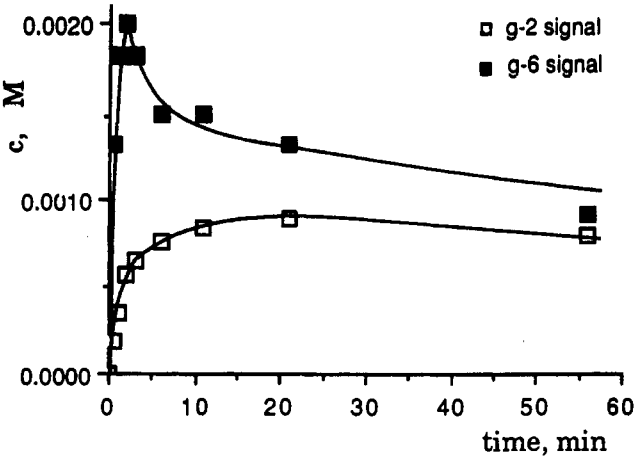

Figure 4. Sample rate data from ESR studies for the two main products of autoxidation (g_6 and first g_2) of $[Fe^{II}(Me,Me,m\text{-xyl})Cl]^+$ in 311APW at dioxygen pressures of 380 Torr and annealing temperatures of 0 °C.

complex forms along the way and has been identified. It is characteristic of those systems that the axial chloride ligand is readily displaced by water or hydroxide. The possible roles of these species relate to the question of whether the duality of ESR-active species may arise from the coordination of the peroxo ligand both inside and outside the cavity even when the axial base position is occupied by the stronger ligand pyridine. For a solution where the two low-spin species have been generated with PhIO in 311APW, after 5 min at room temperature, signals due to both low-spin species have decreased dramatically in intensity and at about the same rate. In the same time interval, the small residual high-spin signal has also disappeared. If at this point one adds a second equivalent of PhIO to the solution, only one of the species reappears, and at an intensity at least double that originally observed. Neither the other low-spin species nor the high-spin species is generated. One possible interpretation of this bizarre result is that the first cycle of formation and decomposition of peroxo complexes leads to replacement of extra-lacunar axial ligands by water molecules and that these then react selectively with PhIO to form only the one low-spin peroxo complex in the second cycle. Further, if the original solution, containing 1 equiv of PhIO and iron complex, were allowed to stand at room temperature for 15 min prior to the second addition of PhIO, then no ESR signals were generated. The latter observation suggests that the μ-oxo-dinuclear complex forms and does not react with PhIO to give one of the original peroxo complexes.

Further Mechanistic Indications. Attempts have been made to use the characteristic ESR spectra to follow the kinetics of formation of the intermediates during the autoxidation of the iron(II) cyclidene complexes. Figure 4 shows sample rate data for the two main products at a dioxygen pressure of 380 torr and a temperature of 0 °C in APW. As pointed out earlier, the high-spin product whose spectrum occurs in the region around $g = 6$ is readily available from other sources, thereby providing easily accessible standards. As is discussed above, the low-spin spectral patterns near $g = 2$ have been reproduced by a variety of reactions and solutions prepared by reaction of the iron(III) complex with H_2O_2 were used as standards to estimate the concentrations of the low-spin products.

Bearing in mind the lack of precision of these rate estimates, it has still been possible to record a number of very helpful observations. The concentration of the low-spin product continues to grow during autoxidation until a plateau is reached after about 10 min. The concentration of the high-spin product reaches a maximum after the first few minutes and then decreases to an almost constant value.[37] The concentration changes for the high- and low-spin species appear to reach their approximately constant values at about the same time, and the long-term concentration of the high-spin complex appears to exceed that of the low-spin complex, but only by a small amount. Also, the early rate of formation of the high-spin species is faster than that of the low-spin complex. Further, at least in some cases, the eventual decrease in concentration of the high-spin complex approximates the time scale for formation of the low spin complex (see Table IV). All of this permits the obvious possibility that the high-spin complex exists along the pathway to the low-spin species.

Table IV. Rate Estimates from ESR Experiments (for 0 °C)

p_{O_2}, Torr	$\tau_{1/2}$,[a] min	$\tau_{1/2}$,[b] min	p_{O_2}, Torr	$\tau_{1/2}$,[a] min	$\tau_{1/2}$,[b] min
12.7	>15		200	ca. 3	ca. 3
38	ca. 5	ca. 3	380	2–3	ca. 3
100	ca. 6	ca. 3	760	ca. 5	ca. 3

[a] From disappearance of high-spin ESR spectrum near $g = 6$. [b] From formation of (low-spin) ESR spectrum of $Fe^{III}(O_2^{2-})$.

There are a variety of pathways that might produce the low spin species, three of which are presented in eqs 8–11. Direct

$$Fe^{II} + HO_2 \rightarrow Fe^{III}(HO_2^-) \quad (8)$$

$$Fe(O_2) + HO_2 \rightarrow Fe^{III}(HO_2^-) + O_2 \quad (9)$$

$$Fe^{II} + HO_2 \rightarrow Fe^{III} + HO_2^- \quad (10)$$

$$Fe^{III} + HO_2^- \rightarrow Fe^{III}(HO_2^-) \quad (11)$$

reaction of superoxide with iron(II) could involve inner sphere redox and formation of iron(III)(HO_2^-) as shown in eq 8. Similarly, the dioxygen adduct of iron(II) could undergo electron transfer with superoxide ion, producing the peroxo complex and a molecule of dioxygen (eq 9). In both cases, one would not expect to correlate a decrease in the concentration of high-spin iron(III) with the formation of the low-spin peroxo complex. The third pathway involves outer-sphere electron transfer between superoxide ion and iron(II), producing more high-spin iron(III) and the hydroperoxide ion (eq 10). The formation of the peroxo complex occurs independently by reaction of iron(III) with the hydroperoxide ion that is formed (eq 11). The latter path explains the fact that the high-spin complex forms faster than does the low-spin complex. Also, it explains why the concentration of the high spin complex of iron(III) first increases rapidly and then decreases while that of the low-spin iron(III) only increases. The stoichiometry is also supportive of this view. Since 2 mol of iron(III) are formed for each mole of hydroperoxide, the concentration ratio, low spin:high spin, cannot exceed 1:1. Finally, some excess of high-spin complex would be expected because catalytic decomposition of peroxide would compete with peroxo complex formation, especially at early times when iron(II) is in large excess. We have refrained from making any direct comparisons between the rates measured by UV–vis studies and those estimated by using ESR spectroscopy because the conditions for the experiments were quite different. While UV–vis data were obtained under pseudo-first-order conditions of constant dioxygen pressure, this cannot be assured for our ESR data because those solutions were only saturated with O_2 at the beginning, and also much higher concentrations of Fe were used.

A thermodynamic argument supports the addition of eq 10 to the mechanism for autoxidation of the iron(II) cyclidene complexes. As pointed out elsewhere,[22] the one-electron-transfer reactions between dioxygen and these iron(II) cyclidene complexes

(37) The relatively fast formation of the high-spin species occurs mainly within the time required to initiate the UV–vis experiments by bubbling O_2 into the solutions (ca. 180 s). This probably contributes to the observed deviations from first-order behavior for some of the rate data (vide supra). Interestingly the formation of the high spin product is fast for low and high dioxygen pressures, but seems to be up to a factor of about 2 slower for intermediate pressures, in parallel with the discrepancies in the UV–vis investigations.

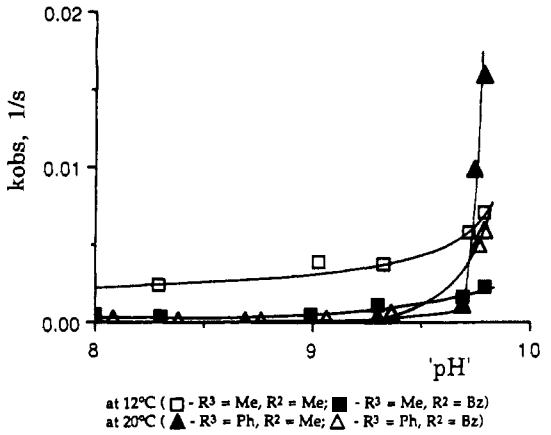

Figure 5. pH dependence (addition of HCl) on the rates of autoxidation of $[Fe^{II}(R^3,R^2,m\text{-xyl})Cl]^+$ in 311APW, 760 Torr of O_2.

are not expected to be thermodynamically favored. Further, Stanbury, Haas, and Taube[19] have shown how the superoxide produced by such a reaction can drive the autoxidation reaction by reacting with a second mole of reductant. Therefore it is proposed that eq 10 be added to the electron-transfer mechanism as an essential step that provides the thermodynamic driving force. Justification for the formulation of the product of the reaction has already been presented.

The alternative bimolecular disproportionation of superoxide is not likely, and the following argument is based on that given by Stanbury, Haas, and Taube.[19] The systems under study relate to highly basic media with pH values that fall in the range above 8. The effective second order superoxide disproportionation rate constant is probably 10^4–10^5 M^{-1} s^{-1}, and the concentration of superoxide is small. $Fe(CN)_6^{4-}$ reacts with superoxide with a rate constant of 3×10^4 M^{-1} s^{-1}, but $[Fe(Me,Me,m\text{-xyl})py]^{2+}$ should react substantially faster because the iron(II,III) cyclidene potential is substantially more cathodic (–0.40 V vs Fc = +0.01 vs NHE in MeOH containing 0.05 M LiCl for $[Fe(Me,Me,m\text{-xyl})Cl]^+$), and the iron(II,III) self exchange rate constant (5.2×10^7 M^{-1} s^{-1}), recalculated based on the newer potential[38] and the measured cross exchange rate between $Co^{III}(phen)_3^{3+}$ and $[Fe(Me,Me,m\text{-xyl})Cl]^{2+}$ in MeOH containing 0.05 M LiCl[39] exceeds that of ferrocyanide by a factor of about 5000. Therefore the reaction between the iron(II) cyclidene complex and superoxide should be much faster than the second-order disproportionation. The above reasoning is based on the MeOH/LiCl solvent system, because both the cross exchange rates and relatively reversible electrochemical potentials were obtained for that system.[40]

Substituent Effects on Autoxidation of $[Fe(R^3,R^2,m\text{-xyl})Cl]^+$ (R^3 = Me, Ph; R^2 = Me, Bz). The influence of the substituents R^2 and R^3 (see structure I) on the rates of autoxidation of these complexes is remarkable. Results are given here for studies in the 311APW system. In all cases, the dioxygen dependence of the rates (average of results at 520 and 650 nm) obeys a saturation law for unbuffered systems at temperatures up to 0 °C and the data have been treated according to eq 6. The original rate constants are reported for a variety of conditions in Table I and the derived kinetic parameters are given in Table II. If the APW system is examined in detail, it becomes clear that the conditions have to be specified closely, if comparisons are to be made between the four complexes listed in the table. Adding only small amounts of acid (ca. 1×10^{-4} M HCl to a solution containing 2.5 M pyridine) changes the autoxidation rates significantly, especially for the Phenyl substituted complexes. Figure 5 shows the effect of added acid; a hypothetical pH value, ignoring the effect of acetone, is calculated for purposes of comparison.

The rate is only weakly sensitive to pH changes at lower pH values (7–9) but changes drastically above a certain pH limit, about pH 9.5–10.0. In the absence of added acid, base, or buffers, the effective pH value for the APW system lies above that limit, so it becomes necessary to compare rates for an extended pH region in order to look for structural effects on the susceptibility toward autoxidation of these dioxygen carriers. Otherwise small changes in the pH of the solvent, originating mainly in different drying methods, might have a dominating effect on the measured rates.

Table II summarizes the kinetic parameters calculated from the oxygen pressure dependence for autoxidations in APW. The p_{O_2} dependencies were obtained under two conditions: pure solvent at 0 and at 25 °C in the presence of 2×10^{-4} M HCl. All complexes show saturation behavior in the unbuffered systems at 0 °C, and the calculated K_{O_2} values agree well with those obtained by extrapolation. On the other hand the p_{O_2} dependencies measured at the higher temperature for the "buffered" systems do not show saturation behavior in the dioxygen pressure range studied (up to 760 Torr), but can rather be approximated by a linear fit, yielding corresponding second-order rates of 1.1×10^{-5}, 2.2×10^{-6}, 6.8×10^{-7}, and 4.0×10^{-7} $Torr^{-1}$ s^{-1} for MeMe, MeBz, PhMe, and PhBz respectively (but with an appreciable intercept for MeMe, MeBz, and PhBz). According to eq 6 the observed autoxidation rates are expected to show a linear dependence on the oxygen pressure at higher temperatures, where K_{O_2} becomes so small that $K_{O_2} * p_{O_2} \ll 1$. The observed behavior is consistent with expectation except for the case of the MeMe complex at 25 °C, where the extrapolated K_{O_2} is associated with the greatest uncertainty, since it is based on only two measured values.

Replacing methyl groups by phenyls in the R^3, or benzyls in the R^2 positions, has the definite effect of lowering the rate constants k', with the doubly substituted complex exhibiting the lowest rate constant. The effect is more profound on substitution of the R^3 group, and substitutions on R^2 and R^3 do not seem to be additive.

Summary

The autoxidation, in APW, of all of the iron(II) cyclidene complexes investigated here can be modeled by an electron-transfer mechanism involving the competitive formation of the dioxygen adduct. Thermodynamic considerations and the nature of the products of the autoxidation strongly support the inference that the autoxidation reaction is driven by a subsequent reaction of the superoxide, that is formed in the primary electron transfer event. A remarkable product of the autoxidation reaction, explicitly identified for $R^2 = R^3$ = Me, is the (peroxo)iron(III) species, which can even be observed at ambient temperatures. Its ESR properties (low spin with g values around 2 and an extremely small anisotropy) are closely similar to those of peroxo complexes in natural systems, and in contrast to the first reported model systems. This species can be generated by five independent routes (autoxidation; $FeO_2 + e^-$; Fe(II) + KO_2; Fe(III) + H_2O_2; Fe(III) + C_6H_5IO) in basic media. The latter route is a rare example of O–O bond formation, which also emphasizes the relevance of these systems as cytochrome P450 models.

Acknowledgment. The authors would like to thank the National Science Foundation for financial support.

(38) These potentials were measured against an internal standard and are therefore more accurate than previously reported ones that were measured against external standards, since junction potentials have now been eliminated.

(39) Kim, S. Ph.D. Thesis, The Ohio State University, 1989.

(40) The cyclidene potential is irreversible up to scanrates of 1000 mV/s in the APW solvent, due to coordination of different axial bases to the electroactive species. Indicated are coordination of pyridine for the Fe(II) species (implicated by negative shift, compared to a system without pyridine, of $E^{\circ\prime}$ to –0.20 V vs NHE) and coordination of OH to the Fe(III) species ($E^{\circ\prime}$ = +0.04 V vs NHE), as was already substantiated by ESR measurements (vide supra).